Preprints of the 19th World Congress
The International Federation of Automatic Control
Cape Town, South Africa. August 24-29, 2014

Extremum Seeking Control With Adaptive Disturbance Feedforward

Sava Marinkov * **Bram de Jager** * **Maarten Steinbuch** *

* *Department of Mechanical Engineering, Eindhoven University of Technology, P.O. Box 513, 5600 MB Eindhoven, The Netherlands, (e-mail: {s.marinkov,a.g.de.jager,m.steinbuch}@tue.nl)*

Abstract: This paper presents an extension to the classical gradient-based extremum seeking control for the case when the disturbances responsible for changes in the extremum of a selected performance function are available for measurement. Based on these additional measurements, an adaptive extremum seeking disturbance feedforward is designed that approximates the unknown, static mapping between the disturbances and the optimal inputs. For this purpose, orthogonal, multivariate Tchebyshev polynomials are used. The feedforward enables the extremum seeking to be conducted in the proximity of the extremum thus yielding improvements both in terms of accuracy and increased convergence speed compared to the traditional scheme. Simulation results given for a turbine driven electrical generator system demonstrate the benefits of the presented design.

Keywords: Extremum seeking control; Feedforward control; Adaptive algorithms.

1. INTRODUCTION

In a wide variety of control applications the aim is to operate a physical system or a process in the vicinity of an extremum (optimal set-point) of some performance function. Very often the performance function is measurable but unknown to the designer, in terms of its exact analytical dependency on the system parameters (optimizing inputs). In such cases Extremum Seeking Control (ESC) techniques can be used to achieve and maintain the operation of a system under optimal conditions. Numerous reports of successful implementations of ESC can be found in literature, *e.g.,* for improving continuously variable transmission efficiency as in Van der Meulen et al. [2012], or for Maximum Power Point Tracking (MPPT) in photovoltaic (PV), fuel cell and wind energy systems, see Zazo et al. [2012], Bizon [2010] and Pan et al. [2008], respectively.

Extremum Seeking Control was first investigated in the 1950s and 1960s as a control framework for finding a minimum or a maximum value of a static map, see Tan et al. [2006]. However, a rigorous stability proof for the "classical" ESC with a general nonlinear dynamical plant arrived only at the beginning of the past decade, see Krstić and Wang [2000]. Since then there has been a revival of interest and a steady development in the field. Today ESC encompasses various online optimization techniques which can roughly be split into gradient-based as in Krstić and Wang [2000], and gradient-free methods, *e.g.,* sliding mode ESC as in Korovin and Utkin [1974]. However, hybrid algorithms such as the Simplex Guided ESC by Zhang and Gans [2012] – a combination between a local, gradient-based search and a global, gradient-free direct search algorithm, also do exist. Furthermore, one can distinguish between numerical optimization-based, parametric and classical-gradient ESC. The classical gradient-based approach, as in Krstić and Wang [2000], Moura and Chang [2010] and Van de Wouw et al. [2012], is the most popular of all ESC schemes due to its simple implementation and a proof of local convergence. It relies on the fact that a signal proportional to the local gradient of the performance function (w.r.t. to the optimizing input) can be extracted from a product between the sinusoidal input perturbation and the resulting system's response. A simple integration of the gradient estimate (or its negation) is then sufficient to continuously steer the system toward the extremum.

Overall, the classical gradient-based ESC schemes demonstrate good seeking behavior when the extremum is static. However, often the optimal operating point can also change over time. For instance, shifts in solar irradiation and wind speed can cause fluctuations in the optimal PV voltage and the optimal wind turbine rotation speed, see Kumari and Babu [2012] and Munteanu et al. [2009]. To account for such variations in the extremum, Krstić [2000] proposed an extension to the original algorithm by introducing a dynamic compensator into the extremum seeking loop. Still, the solution applies only for the case of changes with known dynamics that can be captured by a linear time-invariant system (*e.g.,* a double integrator).

However, in some practical applications the disturbances leading to changes in the optimal input/extremum value of a selected performance function are measurable. In this paper, we show how this additional information can be used to achieve faster and more accurate convergence of the classical gradient-based ESC scheme. In particular, we use the classical gradient-based ESC both to search for a new extremum and to identify the mapping between the disturbances and the optimal inputs. The mapping is approximated by means of multivariate Tchebychev polynomials whose coefficients are adaptively updated using the latest estimate of the optimal input. Based on the approximate mapping, the proposed solution, *i.e.,* the Adaptive disturbance feedforward ESC (AESC), is able to conduct the search in the close vicinity of the ever-changing extremum. This in turn shortens the convergence times and improves the overall extremum tracking performance. Note that the proposed method is not limited to the classical-gradient ESC but can also be used in combination with other similar ESC algorithms, such as

Copyright © 2014 IFAC

those by Ghaffari et al. [2012], Moase et al. [2010] and Moase and Manzie [2012].

In summary, the main contributions of this paper are as follows. The paper presents a solution to the problem of tracking an unknown, time-varying extremum of a certain performance function. This is achieved by extending the original classical gradient-based ESC scheme with an adaptive disturbance feedforward based on multivariate Tchebychev polynomials. The extension greatly enhances the extremum tracking performance as demonstrated in a turbine driven electrical generator system case study.

This paper is organized as follows. Section II provides the problem formulation, followed by the description of the proposed ESC scheme in Section III. Section IV contains representative simulation results from the case study on a turbine driven electrical generator system. Finally, the main conclusions are given in Section V.

2. PROBLEM FORMULATION

Consider a stable dynamical nonlinear closed-loop system:

$$\begin{aligned} \dot{x} &= f(x, q, \theta), \\ y &= h(x), \end{aligned} \tag{1}$$

with continuously differentiable $f : \mathbb{R}^n \times \mathbb{R}^l \times \mathbb{R} \to \mathbb{R}^n$ and $h : \mathbb{R}^n \to \mathbb{R}$. Here $x \in \mathbb{R}^n$ denotes the closed-loop state, $y \in \mathbb{R}$ the *measurable* performance function output, $q \in \mathbb{R}^l$ the *measurable* state disturbance and $\theta \in \mathbb{R}$ denotes a scalar (optimizing) input to the closed loop system.

Let the following assumptions hold:

Assumption 1. The relative degree of (1) w.r.t. the output y and the input θ is at least 1.

Assumption 2. There exists a smooth function $s : \mathbb{R} \times \mathbb{R}^l \to \mathbb{R}^n$ such that $f(x, q, \theta) = 0$, if and only if $x = s(\theta, q)$.

Assumption 3. For each $\theta \in \mathbb{R}$ and $q \in \mathbb{R}^l$, the equilibrium of the system (1), given by $x = s(\theta, q)$, is locally exponentially stable uniformly in θ and q.

Assumption 4. There exists a smooth function $z : \mathbb{R}^l \to \mathbb{R}$ such that for each $q \in \mathbb{R}^l$

$$\begin{aligned} &\frac{\partial h(s(\theta, q))}{\partial \theta}(\theta^*, q) = 0, \\ &\frac{\partial^2 h(s(\theta, q))}{\partial \theta^2}(\theta^*, q) = W(q) < 0, \qquad W(q) = W(q)^T, \end{aligned} \tag{2}$$

if and only if $\theta^* = z(q)$, see Fig. 1 for illustration. Without loss of generality we thus assume that the extremum of h (w.r.t. θ) is a maximum.

The first assumption removes the possibility of a direct relation between the optimizing input and the performance function output (feedthrough). If omitted, the existence of such a relation would cause the related ESC to optimize it instead of the equilibrium performance of the closed-loop system, which is clearly undesirable. The second relates the equilibria of the system to the input and the disturbance while the third provides guarantees for their stability. Finally, the last assumption requires that there is an equilibrium where the performance function admits a maximal (optimal) value for every value of the disturbance. It also states that the corresponding optimizing input is parameterized by the disturbance. Thus one can proceed with construction of an extremum (optimum) seeking algorithm, with a disturbance feedforward. Note that each of the functions f, s, h and z may be unknown to the designer.

Within this class of systems we treat a problem of finding the input $\theta = \theta^*$ which optimizes the performance function $h(s(\theta, q))$ for each value of the measured disturbance q. In particular, we are interested in the ESC-based solutions yielding an approximation of the unknown mapping $z(q)$.

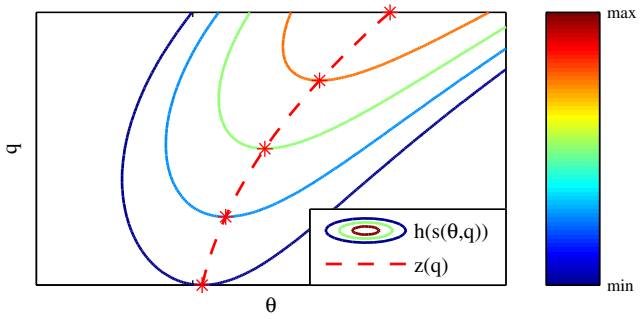

Fig. 1. Illustrations of $h(s(\theta, q))$ and $z(q)$ functions

3. PROPOSED SCHEME

The proposed ESC scheme consists of a performance function feedback and a disturbance feedforward component, see Fig. 2. The feedforward component implements an approximation of the unknown static relation $z(q)$. It computes the feedforward input $\theta_{ff} \in \mathbb{R}$ as a function of the disturbance q and the adaptive feedforward parameters $\eta \in \mathbb{R}^r$. Ideally, one would find the latter by minimizing the norm of the difference between the optimal and the feedforward input. However, as the optimal input θ^* is inherently unknown η is continuously updated using the "best guess" instead, *i.e.,* the (unperturbed) input $\bar{\theta} \approx \theta^*$ to the closed-loop system:

$$\bar{\theta} = \bar{\theta}_{fb} + \theta_{ff}, \tag{3}$$

where $\bar{\theta}_{fb} \in \mathbb{R}$ represents the unperturbed feedback input produced by the feedback component as a result of the application of the classical gradient-based ESC algorithm of Krstić and Wang [2000].

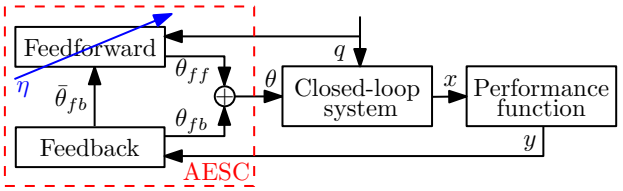

Fig. 2. Adaptive disturbance feedforward ESC

In other words, the feedforward parameters are found by minimizing the square of the approximation error $e \in \mathbb{R}$ given by:

$$e = \bar{\theta} - \theta_{ff} = \bar{\theta}_{fb}. \tag{4}$$

The input θ is a sum of the (perturbed) feedback and the feedforward input, θ_{fb} and θ_{ff}:

$$\theta = \theta_{fb} + \theta_{ff}, \tag{5}$$

where the feedback input is obtained by adding a sinusoidal perturbation signal $\delta = \alpha \sin(\omega t)$ to $\bar{\theta}_{fb}$:

$$\theta_{fb} = \bar{\theta}_{fb} + \delta. \tag{6}$$

Here $\alpha \in \mathbb{R}$ and $\omega \in \mathbb{R}$ denote the perturbation amplitude and frequency.

3.1 Extremum Seeking Feedback Control

The structure of the Extremum Seeking (ES) feedback controller is depicted in Fig. 3. It is shown that the unperturbed feedback input is computed by integrating the approximate gradient $g \in \mathbb{R}$ (w.r.t. θ) of the performance function $h(s(\theta), q)$, *i.e.,* it holds:

$$\dot{\bar{\theta}}_{fb} = K \cdot g, \tag{7}$$

with $\bar{\theta}_{fb}(0) = 0$. Thus a positive adaptation gain $K \in \mathbb{R}$ will result in θ_{fb} that tends to maximize y whereas the negative values will tend to minimize it. The approximate

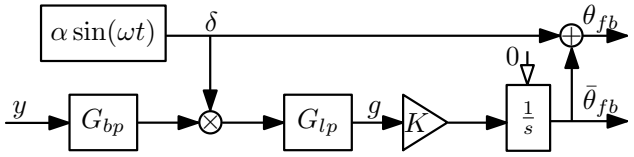

Fig. 3. ES Feedback Controller

gradient g is extracted from the performance function measurement using a well-known procedure that is in the core of the classical gradient-based ESC algorithm of Krstić and Wang [2000] and is given [1] by

$$g = G_{lp}(s)\left[G_{bp}(s)\left[y\right] \cdot \delta\right], \tag{8}$$

where $G_{lp}(s) = \frac{\omega_l}{s+\omega_l}$ represents a low-pass, $G_{bp}(s) = \frac{s(\omega_{l1}+\omega_{h1})}{(s+\omega_{l1})(s+\omega_{h1})}$ a band-pass filter, and $\omega_l, \omega_{l1}, \omega_{h1}$ the related filter cut-off frequencies.

3.2 Extremum Seeking Feedforward Control

In the following subsection the structure of the ES feedforward controller is elaborated in detail, see Fig. 4. In particular, the specific choices for its parametrization and the related parameter estimation are treated.

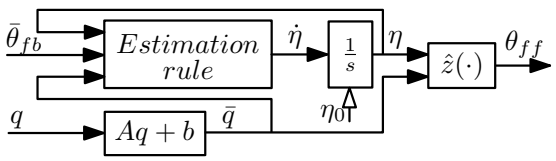

Fig. 4. ES Feedforward Controller

Multivariate Polynomial Approximation. Denote with $q_{min,j}$ and $q_{max,j}$ respectively the minimum and maximum bound of q_j, $j \in \{1, \ldots, l\}$. Furthermore, let $\bar{q} \in [-1, 1]^l$, $\bar{q} = Aq + b$ be the normalized disturbance, where $A \in \mathbb{R}^{l \times l}$ is a diagonal matrix with diagonal entries $A(j,j) = \frac{2}{q_{max,j} - q_{min,j}}$ and $b \in \mathbb{R}^l$ is a vector with elements $b(j) = -\frac{q_{max,j}+q_{min,j}}{q_{max,j}-q_{min,j}}$, $j \in \{1, \ldots, l\}$. Also define $\bar{z} : [-1, 1]^l \to \mathbb{R}$, $\bar{z}(\bar{q}) = z(q)$.

The feedforward input is then computed by approximating the unknown function $\bar{z}(\bar{q})$ by means of a multivariate polynomial $\hat{z} : [-1, 1]^l \times \mathbb{R}^r \to \mathbb{R}$ of degree $c \in \mathbb{N}_0$, *i.e.,*

$$\theta_{ff} = \hat{z}(\bar{q}, \eta). \tag{9}$$

[1] A transfer function in front of a bracketed time function, such as $G(s)[u(t)]$, means a time-domain signal obtained as an output of $G(s)$ driven by $u(t)$, as used by Krstić [2000].

In other words,

$$\bar{z}(\bar{q}) \approx \hat{z}(\bar{q}, \eta) = H^T(\bar{q})\eta, \tag{10}$$

where η is a parameter vector of $r = \frac{(l+c)!}{l!\,c!}$ unknown coefficients and $H(\bar{q}) = [h_1(\bar{q}), \ldots, h_r(\bar{q})]^T$ a vector of multivariate polynomial terms (regressors) $h_i(\bar{q}) : [-1, 1]^l \to \mathbb{R}$, $i \in \{1, \ldots, r\}$. The latter can be formed as a product of different univariate polynomials in $\bar{q}_j$, $j \in \{1, \ldots, l\}$.

In particular, in this work the univariate Tchebychev polynomials of the first kind $T_k(\bar{q}_j)$, $k \in \{0, \ldots, c\}$ are used. They offer a number of computational advantages w.r.t. the other polynomials (*e.g.,* monomials) such as better numerical conditioning in the related parameter estimation algorithms, see Mason and Handscomb [2003]. These polynomials are orthogonal on the interval $[-1, 1]$ and can be constructed using the following recurrence relation:

$$T_{k+1}(\bar{q}_j) = 2\bar{q}_j T_k(\bar{q}_j) - T_{k-1}(\bar{q}_j), \tag{11}$$

where $T_0(\bar{q}_j) = 1$ and $T_1(\bar{q}_j) = \bar{q}_j$, $j \in \{1, \ldots, l\}$.

The regressors h_i, $i \in \{1, \ldots, r\}$ can then be written as:

$$h_i(\bar{q}) = \prod_{j=1}^{l} T_{v_{i,j}}(\bar{q}_j), \tag{12}$$

where the indexes $v_{i,j} \in \mathbb{N}_0$ satisfy:

$$\begin{aligned} v_{i,j} &\in \{0, \ldots, c\}, \\ \sum_{j=1}^{l} v_{i,j} &\leq c, \\ [v_{i_1,1}, \ldots, v_{i_1,l}]^T &\neq [v_{i_2,1}, \ldots, v_{i_2,l}]^T, \end{aligned} \tag{13}$$

$\forall i_1, i_2 \in \{1, \ldots, r\}$.

Parameter estimation. As the feedforward parameters η enter the feedforward function $\hat{z}(\bar{q}, \eta)$ linearly (10), there exists a range of adaptive techniques that can be used for their estimation, see Astrom and Wittenmark [1994]. Here, the **sparse normalized gradient** method proposed by Gui et al. [2013] is used. It is characterized by the following parameter update rule:

$$\dot{\eta} = P_0 H e - \beta_2 \eta \exp^{-\beta_1 \eta^2}, \tag{14}$$

where $P = P^T \in \mathbb{R}^{r \times r}$ denotes positive definite adaptation rate matrix and $\beta_1, \beta_2 \in \mathbb{R}^+$ certain tuning parameters. The adaptation process is initialized with $\eta(0) = \eta_0 \in \mathbb{R}^r$ and a symmetric, positive definite $P(0) = P_0 \in \mathbb{R}^{r \times r}$. The selected method can effectively reduce the computational complexity and increase the speed of parameter convergence in the case of sparse parameter vectors with a large number of elements. Such situations are very often encountered in practice, *e.g.,* when the polynomial order c is chosen rather large. The **sparse normalized gradient** method is based on finding the parameter values which not only minimize the square of the approximation error but also (approximately) result in a parameter vector with a minimal L_0 norm, *i.e.,* a minimal number of non-zero coefficients.

4. CASE STUDY: TURBINE DRIVEN GENERATOR SYSTEM

In this case study the behaviour of the proposed algorithm is examined in the context of an electrical generator (directly) driven by a high-speed variable geometry

turbine (VGT). The AESC is used to find the optimal reference turbine rotational speed $\omega_{t,r} = \omega^*_{t,r}$ such that the maximum electric power output is achieved. However, it is known that both the optimal input and the maximal electric power are time-varying as a consequence of the changes in the VGT exhaust pressure p_e and the VGT vanes control input u_t. The latter two form a disturbance (q) while $\omega_{t,r}$ constitutes the optimizing input (θ). Note that the value of u_t is known as it represents a signal produced by the external VGT airflow control loop [2], whereas the measurement of p_e can be obtained by means of a suitable air pressure sensor.

4.1 Physical model

The speed of the turbine-generator system can be controlled by manipulating the desired (reference) generator current $i_{g,r}$. However, as the related dynamics of the generator current i_g is typically much faster than the speed dynamics, in the context of speed control the former can be neglected, implying $i_g = i_{g,r}$. Thus, assuming that the generator (braking) torque T_g is proportional to its current, the following holds:

$$\dot{\omega}_t = \frac{1}{J}\left(T_d(\omega_t, u_t, p_e) - k_T i_{g,r}\right), \tag{15}$$

where J is the rotor inertia, k_T the generator torque constant and T_d the unknown turbine driving torque. The torque is given by

$$T_d = P_d/\omega_t, \tag{16}$$

where P_d denotes the VGT turbine delivered power, modeled [3] as:

$$P_d = \eta_{tm}\dot{m}_t c_p \upsilon_i \left(1 - (p_e/p_i)^{\frac{\kappa-1}{\kappa}}\right) - B\omega_t^2, \tag{17}$$

$$\eta_{tm} = \eta_{tm,max} - c_{m1}(\omega_t - c_{m2})^{c_{m3}}(BSR - BSR_{opt})^2,$$

$$BSR = r_t\omega_t \left(2c_p\upsilon_i\left[1 - (p_e/p_i)^{\frac{\kappa-1}{\kappa}}\right]\right)^{-0.5},$$

$$\dot{m}_t = A_{max}\frac{p_i}{\sqrt{R_e\upsilon_i}}\sqrt{1 - (p_e/p_i)^{K_t}}\, f_{vgt},$$

$$f_{vgt} = c_{f2} + c_{f1}\sqrt{1 - ((u_t - c_{vgt2})/c_{vgt1})^2}.$$

Here it is assumed that the turbine is operated in a rated speed range implying that $\omega_t \geq c_{m2}$ and $\eta_{tm} \in [0, \eta_{tm,max}]$, where $\eta_{tm,max} \in [0,1]$ and $c_{m2} \in \mathbb{R}^+$. The chosen parameter values are listed in Table 1.

It can be shown that for each pair of p_e and u_t values, there exists an optimal speed $\omega_t = \omega^*_{t,r}$ for which the turbine power is maximal $P_d = P^*_d$. This is illustrated in Fig. 5 and Fig. 6 which show the results of numerical computation of $P_d(\omega_{t,r})$, P^*_d and $\omega^*_{t,r}$ for the specified system parameter values. Thus P_d constitutes a valid choice for the performance function y. Note that one may be tempted to use the instantaneous electric power $P_g = i_{g,r}v_g$ for this purpose instead since in the equilibrium, given by $\omega_t = \omega_{t,r}$ and $\dot{\omega}_t = 0$, the two powers are equivalent, *i.e.*, $P_g = \frac{k_\omega}{k_T}P_d$. Here $v_g = k_\omega\omega_t$ denotes the generator voltage and k_ω the generator speed constant. However, this would not be a valid choice due to the violation of Assumption 1. This is caused by the fact that $i_{g,r}$ is intended to be the output of a feedback controller acting on the speed error $e_{\omega_t} = \omega_t - \omega_{t,r}$ which will typically contain a feedthrough term – thereby directly introducing the optimizing input $\omega_{t,r}$ into the performance function.

Note that the P_d model introduced above is used for design evaluation only. The identification of its parameter values is in general cumbersome as it requires a specialized experimentation and identification procedure, see Wahlstrom and Eriksson [2011]. This justifies the use of non-model based approaches to turbine-speed optimization, such as the one presented here.

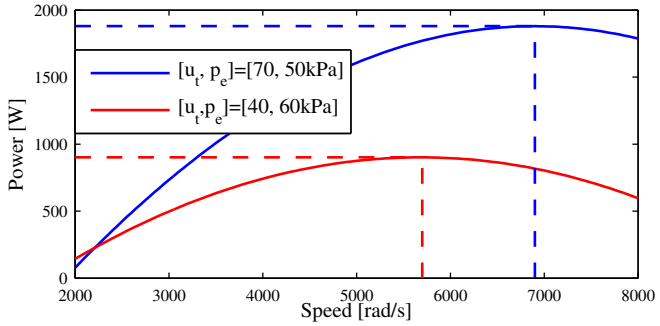

Fig. 5. Turbine delivered power P_d as a function of reference speed $\omega_{t,r}$ for fixed VGT vanes control input u_t and the exhaust pressure p_e

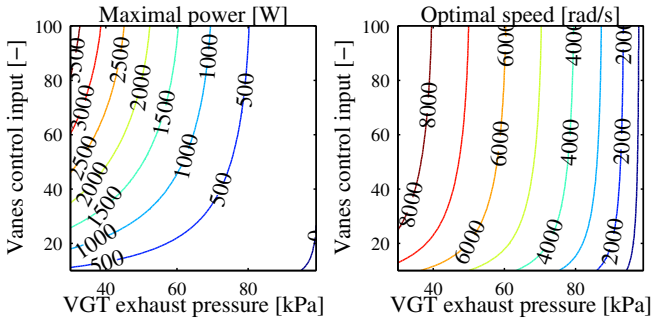

Fig. 6. Optimal delivered power P^*_d and reference speed $\omega^*_{t,r}$ w.r.t. the VGT vanes control input u_t and the exhaust pressure p_e

4.2 Control design

The controller $G_{pid}(s) = 2.4 \cdot 10^{-3}(1 + \frac{31.04}{s} + \frac{-0.96s}{s+90})$ is designed to ensure the closed-loop stability and good reference speed tracking behavior. The overall control scheme is depicted in Fig. 7. As shown, the estimate of the turbine delivered power $\hat{P}_d$ is utilized for the performance function feedback instead of its true value P_d to avoid the need for the measurement of the turbine torque T_d. The estimate $\hat{P}_d$ is obtained by filtering the reference generator current and the measured turbine speed using an observer $G_{kalm}(s) = \left[\frac{10^3}{s^2+200s+2\cdot10^4}, \frac{2s}{s^2+200s+2\cdot10^4}\right]$, *i.e.*,

$$\hat{P}_d = \hat{T}_d\omega_t, \tag{18}$$
$$\hat{T}_d = G_{kalm}(s)[i_{g,r}, \omega_t]^T,$$

where $\hat{T}_d$ denotes the estimated turbine driving torque T_d. The observer constitutes a Kalman filter (see Simon [2006]) designed on the basis of (16). Finally, the AESC

[2] The modeling and control of VGT airflow has not been treated in this paper.
[3] For the details regarding the VGT power model and the explanation of its parameters, see Wahlstrom and Eriksson [2011].

Table 1. Parameter values

AESC	VGT system
$K = 0.7$	$B = 10^{-5}$ [Nms/rad]
$\omega = 8$ [rad/s]	$c_p = 1005$ [J/kg/K]
$\alpha = 60$ [rad/s]	$\kappa = 1.4$
$\omega_l = \frac{\omega}{4}$	$\eta_{tm,max} = 0.82$
$\omega_{h1} = \omega$	$c_{m1} = 1.36$
$\omega_{l1} = 20\omega$	$c_{m2} = 200.14$
$q_{max,1} = 90$	$c_{m3} = 0.01$
$q_{max,2} = 90 \cdot 10^3$ [Pa]	$\omega_{t,0} = 5 \cdot 10^3$ [rad/s]
$q_{min,1} = 10$	$BSR_{opt} = 0.97$
$q_{min,2} = 30 \cdot 10^3$ [Pa]	$r_t = 0.04$ [m]
$c = 2$	$p_i = 100070$ [Pa]
$\eta_0 = [\omega_{t,0}, 0_{1\times5}]^T$	$v_i = 293.15$ [K]
$P_0 = 5 \cdot 10^{-2} I_{6\times6}$	$A_{max} = 1.69 \cdot 10^{-4}$ [m^2]
$\lambda_1 = 1$	$R_e = 287.05$ [J/kg/K]
$\lambda_2 = 0$	$K_t = 2.89$
$\lambda_3 = 0$	$c_{f1} = 1.95$
$\beta_1 = 5 \cdot 10^{-3}$	$c_{f2} = -0.77$
$\beta_2 = 2.5$	$c_{vgt1} = 1.27 \cdot 10^2$
	$c_{vgt2} = 1.17 \cdot 10^2$
	$J = 10^{-4}$ [kgm^2]
	$k_T = 1/20$ [Nm/A]
	$k_\omega = 1/20$ [Vs/rad]

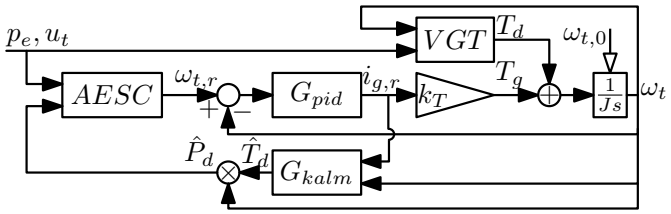

Fig. 7. Turbine driven generator control diagram

has been constructed in a way described in Section 3 using the parameter values listed in Table 1.

4.3 Simulation results

To provide insight in the AESC optimum-tracking behavior the disturbances p_e and u_t are defined in terms of time-varying sinusoids:

$$p_e = 6 \cdot 10^4 - 1.5 \cdot 10^4 \sin(2\pi f_{p_e} t), \qquad (19)$$
$$u_t = 55 - 25 \sin(2\pi f_{u_t} t),$$

where the frequencies f_{p_e} and f_{u_t} change linearly over time, *i.e.*,

$$f_{u_t} = \frac{25}{48 \cdot 10^4} t + \frac{1}{40}, \qquad (20)$$
$$f_{p_e} = \frac{17}{48 \cdot 10^4} t + \frac{1}{200}.$$

In Fig. 8 the results of the AESC application in the context of a high-speed turbine driven electrical generator are shown. From the upper plot it can be seen that the tracking of P_d^* is nearly perfect. Namely, once the ESC feedforward reference speed $\omega_{t,r,ff}$ starts to closely follow the optimal one $\omega_{t,r}^*$, the contribution of the ESC feedback input $\omega_{t,r,fb}$ becomes negligible. This occurs after approximately 200 seconds from the start of simulation where one can observe that $\omega_{t,r,fb}$ starts approaching zero. The time evolution of the related feedforward parameters is given in Fig. 9. Here again the convergence of the feedforward is clearly visible.

For comparison, Fig. 10 presents the case when the traditional ESC is applied to the same problem with the same parameter value settings for the ESC feedback (and also the same inner-loop control). It is immediately apparent that the resulting extremum tracking performance is much poorer than in the first case. In fact, during the simulated time interval the AESC produces significantly less energy loss $E = \int_0^{t_f} (P_d^* - P_d) dt$, dropping from 10 [Wh] in the classical gradient-based ESC to 1.04 [Wh] in the AESC case, or 89.6%.

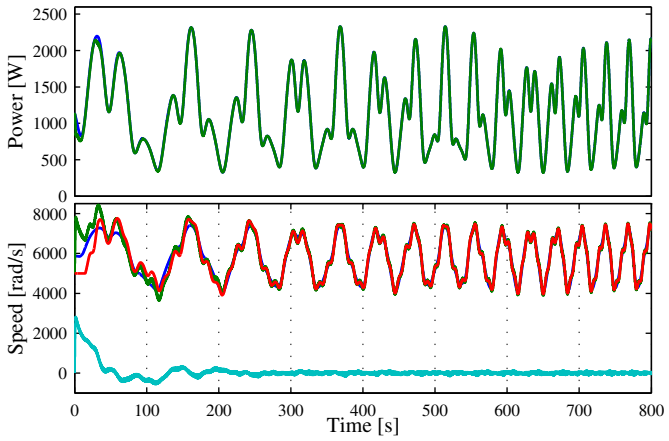

Fig. 8. Simulation results – Adaptive disturbance feedforward ESC (- P_d^*, $\omega_{t,r}^*$; - P_d, ω_t; - $\omega_{t,r,ff}$; - $\omega_{t,r,fb}$)

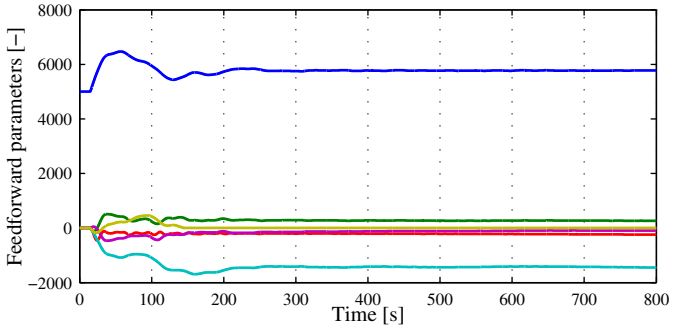

Fig. 9. AESC feedforward parameters η

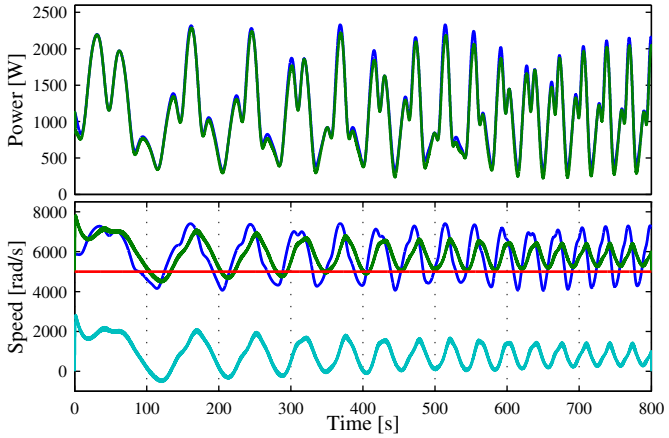

Fig. 10. Simulation results – classical gradient-based ESC (- P_d^*, $\omega_{t,r}^*$; - P_d, ω_t; - $\omega_{t,r,ff}$; - $\omega_{t,r,fb}$)

Finally, Fig. 11 shows the obtained approximate mapping between the optimizing input $\omega_{t,r}^*$ and the disturbances u_t

and p_e (right plot). When compared to the corresponding contour plot from Fig. 6 the resulting map appears a bit inaccurate. One of the reasons for the discrepancy is the fact that the performance function is quite flat in the vicinity of the extremum. Thus large deviations of the reference speed around the optimal value will have very little effect on the resulting performance function value. Nevertheless, when such an approximate optimal speed is substituted in the expression for the delivered power given by (17), together with the corresponding values for p_e and u_t, the resulting power matches the optimal one quite well, as can be seen in the left plot of Fig. 11.

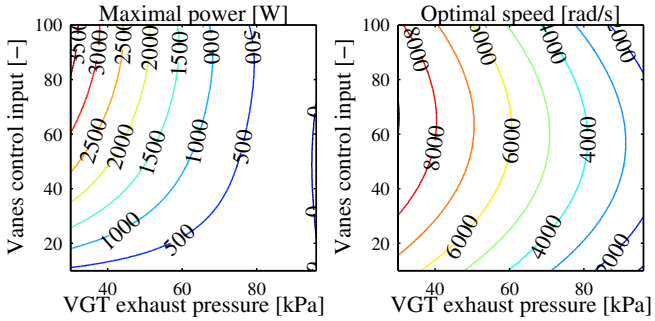

Fig. 11. Feedforward approximation of the optimal delivered power P_d^* and reference speed $\omega_{t,r}^*$ w.r.t. the VGT vanes control input u_t and the exhaust pressure p_e

5. CONCLUSIONS

In this paper a novel Extremum Seeking Control scheme has been presented based on an adaptive disturbance feedforward. The proposed solution achieves significant performance improvements especially in terms of convergence speed and accuracy compared to the original classical gradient-based ESC. This is verified by means of simulations in a turbine driven generator case study. Future work will include a rigorous mathematical analysis of the proposed scheme to provide a theoretical foundation for the claims made in this paper.

REFERENCES

Karl Johan Astrom and Bjorn Wittenmark. *Adaptive Control*. Addison-Wesley Longman Publishing Co., Inc., December 1994.

N. Bizon. On tracking robustness in adaptive extremum seeking control of the fuel cell power plants. *Applied Energy*, 87(10):3115–3130, October 2010.

Azad Ghaffari, Miroslav Krstić, and Dragan Nešić. Multivariable Newton-based extremum seeking. *Automatica*, 48(8):1759–1767, August 2012.

Guan Gui, Wei Peng, and Fumiyuki Adachi. Improved adaptive sparse channel estimation based on the least mean square algorithm. In *2013 IEEE Wireless Communications and Networking Conference (WCNC)*, pages 3105–3109. IEEE, April 2013.

S.K. Korovin and V.I. Utkin. Using sliding modes in static optimization and nonlinear programming. *Automatica*, 10(5):525–532, September 1974.

Miroslav Krstić. Performance improvement and limitations in extremum seeking control. *Systems & Control Letters*, 39(5):313–326, April 2000.

Miroslav Krstić and Hsin-Hsiung Wang. Stability of extremum seeking feedback for general nonlinear dynamic systems. *Automatica*, 36(4):595–601, April 2000.

J Surya Kumari and Ch Sai Babu. Mathematical Modeling and Simulation of Photovoltaic Cell using Matlab-Simulink Environment. *International Journal of Electrical and Computer Engineering*, 2(1):26–34, February 2012.

J. C. Mason and David Christopher Handscomb. *Chebyshev Polynomials*. 2003.

W.H. Moase and C. Manzie. Fast extremum-seeking for Wiener-Hammerstein plants. *Automatica*, 48(10):2433–2443, October 2012.

William H. Moase, Chris Manzie, and Michael J. Brear. Newton-Like Extremum-Seeking for the Control of Thermoacoustic Instability. *IEEE Transactions on Automatic Control*, 55(9):2094–2105, September 2010.

Scott J Moura and Yiyao A Chang. Asymptotic convergence through Lyapunov-based switching in extremum seeking with application to photovoltaic systems. In *American Control Conference 2010*, pages 3542–3548, Baltimore, MD, USA, 2010. IEEE.

Iulian Munteanu, Antoneta Iuliana Bratcu, and Emil Ceang. Wind turbulence used as searching signal for MPPT in variable-speed wind energy conversion systems. *Renewable Energy*, 34(1):322–327, January 2009.

Tinglong Pan, Zhicheng Ji, and Zhenhua Jiang. Maximum Power Point Tracking of Wind Energy Conversion Systems Based on Sliding Mode Extremum Seeking Control. In *2008 IEEE Energy 2030 Conference*, pages 1–5. IEEE, November 2008.

Dan Simon. *Optimal State Estimation: Kalman, H-inf, and Nonlinear Approaches*. John Wiley & Sons, Inc., Hoboken, NJ, USA, May 2006.

Ying Tan, Dragan Nešić, and Iven Mareels. On non-local stability properties of extremum seeking control. *Automatica*, 42(6):889–903, June 2006.

Nathan van de Wouw, Mark Haring, and Dragan Nesic. Extremum-seeking control for periodic steady-state response optimization. In *Proceedings of the 51st IEEE Conference on Decision and Control (CDC)*, pages 1603–1608. IEEE, December 2012.

S. van der Meulen, B. de Jager, F. Veldpaus, E. van der Noll, F. van der Sluis, and M. Steinbuch. Improving Continuously Variable Transmission Efficiency With Extremum Seeking Control. *IEEE Transactions on Control Systems Technology*, 20(5):1376–1383, September 2012.

J. Wahlstrom and L. Eriksson. Modelling diesel engines with a variable-geometry turbocharger and exhaust gas recirculation by optimization of model parameters for capturing non-linear system dynamics. *Proceedings of the Institution of Mechanical Engineers, Part D: Journal of Automobile Engineering*, 225(7):960–986, May 2011.

Héctor Zazo, Esteban del Castillo, Jean François Reynaud, and Ramon Leyva. MPPT for Photovoltaic Modules via Newton-Like Extremum Seeking Control. *Energies*, 5 (12):2652–2666, July 2012.

Yinghua Zhang and Nicholas Gans. Simplex guided extremum seeking control for real-time optimization. In *American Control Conference (ACC), 2012*, volume 2, pages 3377–3382, Montreal, 2012.